

the acridine orange moiety of **1** as an internal, photoactivated "molecular scissors" to map platinum binding sites on  $^{32}\text{P}$ -end-labeled DNA restriction fragments, in a manner complementary to our previous mapping of *cis*-DDP binding to DNA using exonuclease III.<sup>2a,21</sup>

In summary, the intercalator-linked platinum complex **1** has been synthesized in good yield. From its DNA binding and light-activated nicking properties, **1** should prove to be a useful probe of the regioselectivity and stereospecificity of diaminedichloroplatinum(II) binding to DNA. The similarity of **1** to the antitumor drug *cis*-DDP makes it potentially useful for probing aspects of the biological mechanism of action of anticancer platinum compounds.

**Acknowledgment.** This work was supported by U.S. Public Health Service Grants CA 15826 (at Columbia University) and CA 34992 (at MIT) awarded by the National Cancer Institute, Department of Health and Human Services. B.E.B. is a Postgraduate Fellow of the Canadian Natural Sciences and Engineering Research Council. We thank Engelhard Industries for a loan of  $\text{K}_2\text{PtCl}_4$  from which the platinum compounds were synthesized.

(21) Tullius, T. D.; Lippard, S. J. *J. Am. Chem. Soc.* **1981**, *103*, 4620.

### Observation of 1000-fold Enhancement of $^{15}\text{N}$ NMR via Proton-Detected Multiquantum Coherences: Studies of Large Peptides

David H. Live,<sup>1a</sup> Donald G. Davis,<sup>1b</sup> William C. Agosta,<sup>1a</sup> and David Cowburn\*<sup>1a</sup>

The Rockefeller University  
New York, New York 10021  
Adelphi University  
Garden City, New York, 11530

Received May 2, 1984

The severe sensitivity limitations associated with the observation of  $^{15}\text{N}$  NMR signals, especially at natural abundance, make any improvement in sensitivity of considerable importance.<sup>2,3</sup> The potential advantages of using indirect detection via protons for nuclei like  $^{15}\text{N}$  and  $^{13}\text{C}$  over conventional direct detection methods have been recognized,<sup>4-8</sup> but the enhancement has not been explicitly measured.<sup>8</sup> It is important to know if the theoretical enhancement over simple direct detection ( $\gamma_{\text{H}}/\gamma_{^{15}\text{N}}$ ),<sup>3</sup> about 1000-fold, can be achieved, and if so, whether this can be done routinely on samples of interest at natural abundance.

We report here the quantitative determination of the enhancement under typical conditions for biological macromolecules using a 50 mM solution of 2-pyrrolidinone (**1**) in water and also demonstrate the application of this method to an experimentally demanding case, showing chemical shift correlation of amide protons and nitrogen resonances in the 28-residue peptide thymosin

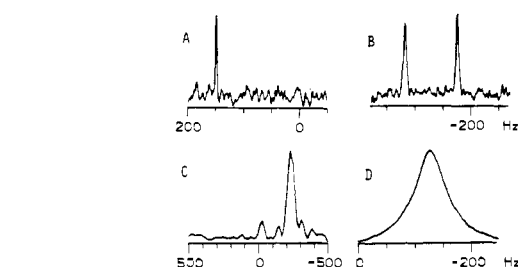


**Figure 1.** Comparison<sup>9</sup> of direct  $^{15}\text{N}$  and indirect proton-detected spectra of pyrrolidinone (**1**) (50 mM, 95% $\text{H}_2\text{O}/5\%\text{D}_2\text{O}$ ). (A) Directly detected INEPT<sup>2,3</sup> spectrum of 20-mm o.d. sample, active volume 10 mL, 2180 scans in 28 min,  $S/N = 9$ . (B)  $^1\text{H}$ -detected  $^{15}\text{N}$  spectrum of **1** taken in a 12-mm tube in a modified 12-mm  $^1\text{H}$  probe, active volume 1 mL, 128 scans in 0.8 min,  $S/N = 11$ . The signals are at the position of the  $^{15}\text{N}$  satellites. (C)  $^{15}\text{N}$  projection of a complete two-dimensional data set for **1**, as in B. Total accumulation time 13 min (16 blocks),  $S/N = 70$ . (D)  $^1\text{H}$  spectrum of **1** using Redfield pulse acquisition.

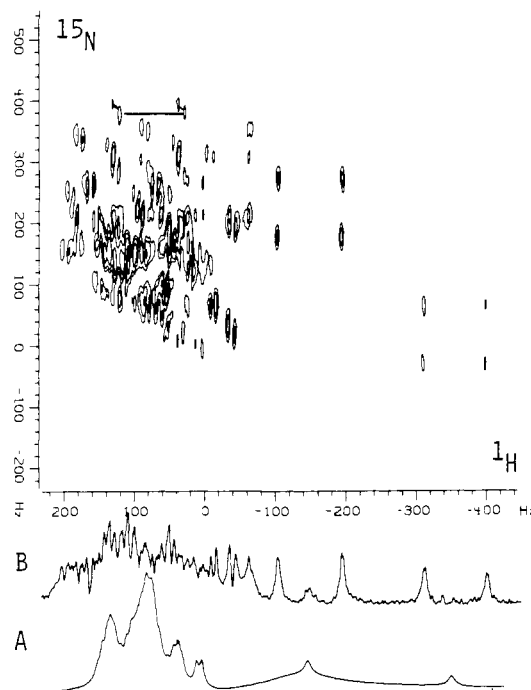


**Figure 2.** Two-dimensional  $^1\text{H}/^{15}\text{N}$  chemical shift correlation for thymosin  $\alpha_1$ , via proton-detected double-quantum (nonconservative) coherence. Sample was 30 mM in 95%  $\text{H}_2\text{O}/5\%\text{D}_2\text{O}$ , at pH 5.4. Total accumulation time about 12 h. The zero-frequency points are the instrumental synthesizer frequencies and correspond to 8.04 ppm (from  $\text{Me}_4\text{Si}$ ,  $^1\text{H}$ ) and 125.3 ppm (from  $\text{NH}_3$ ,  $^{15}\text{N}$ ). Chemical shifts in the  $^{15}\text{N}$  direction are given by  $(\Delta_{\text{H}} - \Delta_{\text{N}})$ , cf. ref 8, for this cycling scheme, and the negative value of  $\gamma_{\text{N}}$ . Each amide proton gives a set of four peaks in the contour plot arising from the large  $^1\text{H}$ - $^{15}\text{N}$  coupling and the smaller coupling of amide to  $\text{H}^\alpha$ . One such set is connected by a line in the upper left. (A) Redfield pulse  $^1\text{H}$  spectrum of the amide region. (B)  $^1\text{H}$  ( $f_2$ ) projection of the two-dimensional data set and a contour plot of the data set. Each amide appears as four lines from couplings to  $^1\text{H}^\alpha$  and to  $^{15}\text{N}$ .

$\alpha_1$  at 30 mM in water. Both samples were at natural abundance for  $^{15}\text{N}$ .<sup>9</sup>

The spectra of **1** with  $^{15}\text{N}$  detection using INEPT<sup>2</sup> and with indirect  $^1\text{H}$  detection of  $^{15}\text{N}$  satellites using multiquantum co-

- (1) (a) The Rockefeller University. (b) Adelphi University.  
(2) Morris, G. A.; Freeman, R. *J. Am. Chem. Soc.* **1979**, *101*, 760-762.  
(3) Morris, G. A. *J. Am. Chem. Soc.* **1980**, *102*, 428-429.  
(4) Aue, P. W.; Bartholdi, W.; Ernst, R. R. *J. Chem. Phys.* **1976**, *64*, 2229-2246.  
(5) Müller, L. *J. Am. Chem. Soc.* **1979**, *101*, 4481-4484.  
(6) Bodenhausen, G.; Ruben, D. *J. Chem. Phys. Lett.* **1980**, *69*, 185-190.  
Freeman, R.; Mareci, T. H.; Morris, G. A. *J. Magn. Reson.* **1981**, *42*, 343-351.  
(7) Redfield, A. G. *Chem. Phys. Lett.* **1983**, *96*, 539-543. Roy, S.; Papastavros, M. Z.; Sanchez, V.; Redfield, A. G. *Biochemistry*, in press.  
(8) Bax, A.; Griffey, R. H.; Hawkins, B. L. *J. Magn. Reson.* **1983**, *55*, 301-312; *J. Am. Chem. Soc.* **1984**, *105*, 7188-7190. Griffey, R. H.; Poulter C. D.; Bax, A.; Hawkins, B. L.; Yamaizumi, Z.; Nishimura, S. *Proc. Natl. Acad. Sci. U.S.A.* **1983**, *80*, 5895-5897.

- (9) The spectra were obtained on an NT-300W spectrometer, with a top-entry probe stack system. For indirect detection experiments, an additional synthesizer-based radiofrequency generator was used. A  $^1\text{H}$  12-mm probe was modified by inclusion of a second coil matched for  $^{15}\text{N}$ . The separate coil eliminates lock interference previously observed by others in single-coil designs<sup>9</sup> (Live, D. H.; Cowburn, D., unpublished results). Sequences used were generally those described previously<sup>8</sup> (Minorette, A.; Aue, W. P.; Reinhold, M.; Ernst, R. R. *J. Magn. Reson.* **1979**, *40*, 175-186) with proton excitation generated by a selective pulse (Redfield, A.; Kunz, J.; Ralph, E. K. *J. Magn. Reson.* **1975**, *19*, 114-119).

herence transfer<sup>5,8</sup> are shown in Figure 1. The signal to noise ratios ( $S/N$ ) of the two spectra are comparable, but the directly detected  $^{15}\text{N}$  spectrum was obtained with 10-fold greater volume of sample and 35-fold longer time. After correction for (a) different acquisition times, (b) relative sample volumes, (c) the INEPT enhancement factor,<sup>10</sup> and (d) the total intensity of the doublets in Figure 1B, the enhancement between the direct and indirect detection is found to be about 1230, compared to the theoretical 961.<sup>11</sup> The  $S/N$  of the  $^{15}\text{N}$  projection of a two-dimensional data set gives a similar value for the sensitivity gain. The line width of the conventional amide proton spectrum of **1** is very broad (Figure 1D), because of  $^{14}\text{N}$  quadrupolar relaxation. The sharpness of the  $^{15}\text{N}$  satellites suggests additionally that much more precise NMR measurements of the proton spectra of amides are possible by this method.

Application of this method to nitrogen and proton NMR of amide resonances of larger peptides in water has considerable potential. Sensitivity is usually at a premium for such materials. The resulting two-dimensional spectra contain the  $^1\text{H}/^{15}\text{N}$  connectivity information, have substantially improved separation of  $^1\text{H}$  signals otherwise at equal shifts, and permit better determination of coupling constants because of the signal separation and because of the narrower lines of  $^{15}\text{N}$  multiplets compared to the  $^{14}\text{N}$  equivalents. These features are illustrated by the spectrum of thymosin  $\alpha_1$ , a peptide implicated in the differentiation of T cells.<sup>12</sup> The conventional proton spectrum of the amide region, including the 28 peptidic amide proton signals, falls within 0.65 ppm, preventing the discrimination of any detail (Figure 2A). The two-dimensional  $^1\text{H}/^{15}\text{N}$  spectrum (Figure 2B) shows a number of clearly resolved  $^3J(\text{H}-\text{H}^\alpha)$  couplings. The analysis of such couplings is important for determining the solution conformation of the peptide.

A further application of this experiment is the sensitive observation of labeled materials, with very high selectivity for the proton attached to the labeled nitrogen. Using this method we have been able to observe the resonance of a single amide proton in a highly overlapped region of more than 100 amide resonances from a protein/peptide complex of 22 000 daltons,<sup>13</sup> at 1.5 mM concentration in 5-min acquisition time. These techniques also present new opportunities for using stable isotope materials in studies of the metabolism of nitrogen, as has been suggested previously for  $^{13}\text{C}$  studies.<sup>14</sup>

The demonstration of a 1000-fold sensitivity increase via heteronuclear multiquantum coherence transfer substantially reduces the restrictions on  $^{15}\text{N}$  NMR arising from low sensitivity for compounds in which such coherence transfer can be obtained.<sup>15</sup> It may be expected that important enhancements, though less dramatic, can be observed for other nuclei (e.g.,  $^{13}\text{C}$ ,  $^{29}\text{Si}$ , and  $^{113}\text{Cd}$ ).

**Note Added in Proof.** Expected enhancements have been experimentally observed for several other nuclei.

**Acknowledgment.** Supported by grants from NIH (AM-20357, GM-24267), NSF (PCM 79-12083), and the Camille and Henry

(10) In theory, the advantage of INEPT should be 10-fold.<sup>2</sup> We achieve experimentally a factor of 8.5.

(11) The third-power dependence on  $(\gamma_{\text{H}}/\gamma_{\text{N}})$  arises from the difference in spin polarization, magnetic moment, and detection frequency of the nuclei. We have neglected adjustments for instrumental effects such as differences in the  $Q$  factors of probes used (Abragam, A. "The Principles of Nuclear Magnetism"; Oxford University Press: Oxford, England, 1961; p 83) or for integrated intensities.

(12) White, A. In "Biochemical Actions of Hormones"; Academic Press: New York, 1980; Vol. VII, pp 1-46. Felix, A. M.; Heimer E. P.; Wang, C.-T.; Lambros, T. J.; Swistok, J.; Ahmad, M.; Roszkowski, M.; Confalone, D.; Meienhofer, J.; Trzeciak, A.; Gillissen, D. In "Peptides; Structure and Function", Proceedings 8th American Peptide Symposium; Hruby, V. J., Rich, D. H., Eds.; 1983; pp 889-898. Shift correlation maps for several smaller peptides have also been obtained.

(13) Live, D. H.; Breslow, E.; Davis, D. G.; Cowburn, D., unpublished results.

(14) Sillerud, L. O.; Alger, J. R.; Shulman, R. G. *J. Magn. Reson.* **1981**, *45*, 142-150.

(15) Bax, A.; Niu, C.-H.; Live, D. *J. Am. Chem. Soc.* **1984**, *106*, 1150-1151.

Dreyfus Foundation. We are grateful to Dr. A. Bax, N.I.H., for preprints of his studies, Dr. Arthur Felix, Hoffmann-La Roche Inc., for thymosin  $\alpha_1$ , and Dr. Craig Bradley, Cryomagnetics Inc., for suggestions on probe modifications.

Registry No. 2-Pyrrolidinone, 616-45-5; thymosin  $\alpha_1$ , 69521-94-4.

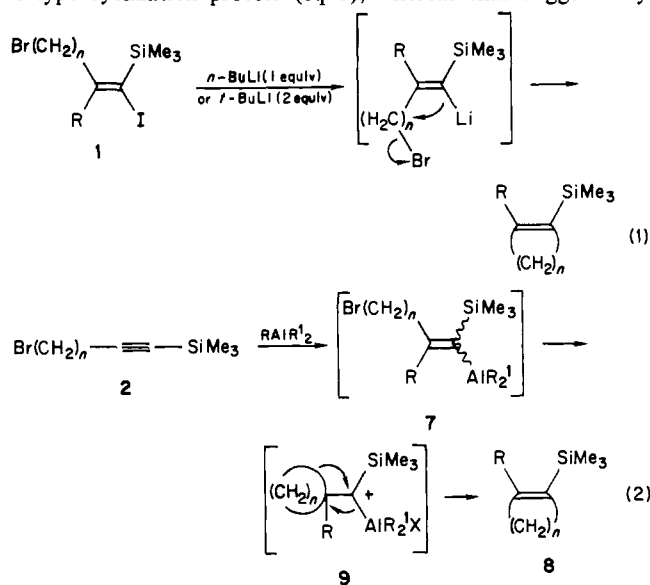
## Mechanistic Duality in Cyclialkylation of Alkenylmetal Derivatives<sup>1</sup>

Larry D. Boardman,<sup>2a</sup> Vahid Bagheri, Hiroyuki Sawada,<sup>2b</sup> and Ei-ichi Negishi\*

Department of Chemistry, Purdue University  
West Lafayette, Indiana 47907

Received June 4, 1984

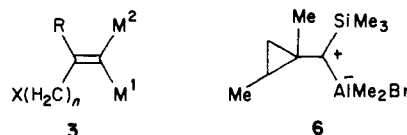
We have recently reported two cyclization reactions proceeding via [1-(trimethylsilyl)-1-alkenyl]metals containing a halogen leaving group.<sup>3</sup> On the basis of the available data, we suggested that the reaction of **1** with either *n*-BuLi or *t*-BuLi might be a  $\sigma$ -type cyclization process (eq 1), whereas that triggered by



a,  $n=2$ ; b,  $n=3$ ; c,  $n=4$ ; R=H or C group; R<sup>1</sup>=C group

treatment of haloalkylsubstituted 1-(trimethylsilyl)-1-alkynes (**2**) with *i*-Bu<sub>2</sub>AlH, Me<sub>3</sub>Al-Cl<sub>2</sub>ZrCp<sub>2</sub>, or Cl(H)ZrCp<sub>2</sub> followed by AlCl<sub>3</sub> might be a  $\pi$ -type cyclization process, e.g., eq 2.

We now present data that not only support the above-mentioned mechanistic duality but reveal some striking differences between the two processes summarized in Table I. Perhaps more significantly, we find that the  $\pi$ -type process is of considerable generality with respect to the two metals of 1,1-dimetalloalkenes (**3**), providing a facile synthesis of cycloalkenylmetals containing



M<sup>1</sup> = Al, Zr, Zn, or Si;  
M<sup>2</sup> = Si, Al, Zn, or Zr;  
R = H or C group;  
X = halogen

metals readily replaceable with various electrophiles, such as halogens.

(1) Metal Promoted Cyclization. 5. Part 4: Miller, J. A.; Negishi, E. *Isr. J. Chem.* **1984**, *24*, 76.

(2) (a) A Proctor and Gamble Fellow. (b) On leave from Ube Industries, Ltd., Ube, Japan.

(3) Negishi, E.; Boardman, L. D.; Tour, J. M.; Sawada, H.; Rand, C. L. *J. Am. Chem. Soc.* **1983**, *105*, 6344.